Neurobiology of Disease

Homer Protein–Metabotropic Glutamate Receptor Binding Regulates Endocannabinoid Signaling and Affects Hyperexcitability in a Mouse Model of Fragile X Syndrome

Ai-Hui Tang (唐爱辉)[1,2] and Bradley E. Alger[1,2]
[1]Department of Physiology and [2]Program in Neuroscience, University of Maryland School of Medicine, Baltimore, Maryland 21201

The Fmr1 knock-out mouse model of fragile X syndrome (*Fmr1*$^{-/y}$) has an epileptogenic phenotype that is triggered by group I metabotropic glutamate receptor (mGluR) activation. We found that a membrane-permeable peptide that disrupts mGluR5 interactions with long-form Homers enhanced mGluR-induced epileptiform burst firing in wild-type (WT) animals, replicating the early stages of hyperexcitability in *Fmr1*$^{-/y}$. The peptide enhanced mGluR-evoked endocannabinoid (eCB)-mediated suppression of inhibitory synapses, decreased it at excitatory synapses in WTs, but had no effect on eCB actions in *Fmr1*$^{-/y}$. At a low concentration, the mGluR agonist did not generate eCBs at excitatory synapses but nevertheless induced burst firing in both *Fmr1*$^{-/y}$ and peptide-treated WT slices. This burst firing was suppressed by a cannabinoid receptor antagonist. We suggest that integrity of Homer scaffolds is essential for normal mGluR–eCB functioning and that aberrant eCB signaling resulting from disturbances of this molecular structure contributes to the epileptic phenotype of *Fmr1*$^{-/y}$.

Key words: DHPG; epilepsy; Fmr1; hippocampus; inhibitory synapses; seizure

Introduction

Fragile X syndrome (FXS) is an autism spectrum disorder accompanied frequently by epileptic seizures. FXS is caused by transcriptional silencing of the gene *Fmr1*, which codes for fragile X mental retardation protein (FMRP; Darnell and Klann, 2013), a translation inhibitor that can be activated by group I metabotropic glutamate receptors (mGluRs; i.e., mGluR1 and mGluR5). Mice lacking *Fmr1* (*Fmr1*$^{-/y}$) have some behavioral abnormalities that mimic those in humans with FXS. According to the mGluR theory of FXS (Bear et al., 2004), the absence of FMRP allows mGluRs to generate excessive protein synthesis, which contributes to FXS pathology (Dölen et al., 2007). Persistent activation of group I mGluRs produces prolonged epileptiform discharges in *Fmr1*$^{-/y}$ mice (Chuang et al., 2005; Zhao et al., 2011; Osterweil et al., 2013). However, the hyperexcitability phenotype in FXS may not be explained by this mechanism alone; decreases in inhibitory transmission also occur in *Fmr1*$^{-/y}$ mice (Olmos-Serrano et al., 2010; Paluszkiewicz et al., 2011).

Activation of group I mGluRs efficiently mobilizes endocannabinoids (eCBs), eCB$_{mGluR}$ (Varma et al., 2001), that suppress transmitter release by stimulating CB$_1$Rs, which are more concentrated on the presynaptic terminals of inhibitory than excitatory cells (Kano et al., 2009). eCB$_{mGluR}$ can cause short-term (Morishita et al., 1998) or long-term (for review, see Heifets and Castillo, 2009) synaptic depression of GABA or glutamate release. In *Fmr1*$^{-/y}$ mice, eCB$_{mGluR}$ at GABA synapses is enhanced in the hippocampus (Zhang and Alger, 2010) and striatum (Maccarrone et al., 2010) because of increased coupling between mGluRs and eCB mobilization.

Homer proteins anchor mGluRs to the postsynaptic density in spines (Klugmann and Szumlinski, 2008). Long-form Homer proteins mediate protein–protein interactions through tetramer formation, which is disrupted by the dominant-negative Homer 1a. Binding or unbinding Homers facilitate a variety of mGluR-dependent biochemical reactions, and, therefore, the Homer system acts as a molecular switch to reprioritize mGluR signaling (Kammermeier, 2008).

In expression systems (Jung et al., 2007) and dissociated cell culture (Roloff et al., 2010), Homer proteins regulate eCB$_{mGluR}$. Interactions between mGluR5 and Homers are decreased in *Fmr1*$^{-/y}$ mice (Giuffrida et al., 2005; Ronesi and Huber, 2008). Manipulations of eCB signaling rescue various aspects of the *Fmr1*$^{-/y}$ phenotype (Jung et al., 2012; Busquets-Garcia et al., 2013). Homer 1a deletion partially reverses the *Fmr1*$^{-/y}$ phenotype (Ronesi et al., 2012), but the hypothesis that Homer proteins regulate eCB$_{mGluR}$ has not been tested.

We investigated (*S*)-3,5-dihydroxyphenylglycine (DHPG)-induced epileptic hyperexcitability in *Fmr1*$^{-/y}$ mice (Chuang et al., 2005; Bianchi et al., 2009), but we used a low DHPG concentration and focused on short epileptiform bursts rather than the longer discharges produced by high concentrations (Chuang et al., 2005). We found that hippocampal slices from *Fmr1*$^{-/y}$ mice,

Received Oct. 30, 2014; revised Jan. 22, 2015; accepted Jan. 29, 2015.
Author contributions: A.-H.T. and B.E.A. designed research; A.-H.T. performed research; A.-H.T. analyzed data; A.-H.T. and B.E.A. wrote the paper.
This work was supported by National Institutes of Health Grant R01 MH077277 and a program grant from the FRAXA Research Foundation (B.E.A.).
The authors declare no competing financial interests.
Correspondence should be addressed to Dr. Ai-Hui Tang, Department of Physiology, University of Maryland, 655 West Baltimore Street, Baltimore, MD 21201. E-mail: tangaihui@gmail.com.
DOI:10.1523/JNEUROSCI.4499-14.2015
Copyright © 2015 the authors 0270-6474/15/353938-08$15.00/0

or wild-type (WT) animals in which Homer interactions were disrupted by a peptide that binds to long Homers, are more excitable than control WT slices. The increased excitability was associated with enhanced eCB_{mGluR} at GABAergic synapses. CB_1R antagonism reversed this epileptic phenotype in *Fmr1*$^{-/y}$ and peptide-treated WT slices. The results contribute to the understanding FXS and eCB signaling and, if extended to humans, could have translational implications.

Materials and Methods

Animals. All experimental protocols were approved by the University of Maryland, Baltimore School of Medicine Institutional Animal Care and Use Committee, and animal handling followed national and international guidelines to minimize the numbers of animals used and mitigate pain or suffering. We used tissue from 4- to 5-week-old male *Fmr1*$^{-/y}$ and age-matched WT mice on the C57BL/6J strain (The Jackson Laboratory). To test the generality of Homer modulation of eCB_{mGluR}, in some experiments, as noted, 5- to 6-week-old male Sprague Dawley rats (Charles River) were used.

Preparation of slices. Animals were deeply sedated with isoflurane and decapitated. Slices, 400 μm thick, were cut on a vibratome (VT1200s; Leica) in an ice-cold extracellular recording solution (ACSF) containing the following (mM): 130 NaCl, 3 KCl, 2.5 $CaCl_2$, 2 $MgSO_4$, 1 NaH_2PO_4, 25 $NaHCO_3$, and 10 glucose, pH 7.4 (bubbled with 95% O_2, 5% CO_2). Slices were stored in a holding chamber on filter paper at the interface of ACSF and a moist, oxygenated atmosphere at room temperature (22°C) for >1 h before transfer to the recording chamber (RC-27L; Warner Instruments).

Electrophysiology. Visualized whole-cell recordings were made with a Nikon E600 microscope. Voltage-clamped CA1 pyramidal cells were filled with the following (mM): 90 $CsCH_3SO_4$, 1 $MgCl_2$, 50 CsCl, 2 MgATP, 0.2 Cs_4-BAPTA, 10 HEPES, 0.3 Tris-GTP, and 5 QX314, pH 7.2 (280–290 mOsm). If the series resistances changed by >20%, the data were discarded. For evoked EPSC (eEPSC) recordings, the $GABA_A$ receptor antagonist picrotoxin (PTX; 100 μM) was present, and a cut between CA3 and CA1 prevented recurrent seizure activity. For eIPSC recordings, NBQX (10 μM) and D-AP-5 (20 μM) were present to block glutamatergic EPSCs. eCB-insensitive perisomatic inhibitory synapses were blocked by >1 h pretreatment with the P/Q-type Ca^{2+}-channel blocker ω-agatoxin GVIA (Wilson et al., 2001; cf. Freund and Katona, 2007; Lenz et al., 1998). eIPSCs or eEPSCs were elicited by 200-μs-long extracellular stimuli delivered at 0.2 Hz with concentric bipolar stimulating electrodes in CA1 or CA3 stratum radiatum. DHPG was applied for 3–4 min when eIPSCs were tested and for 5 min when eEPSCs were tested. To measure the DHPG-induced inhibition, the peak eIPSCs or eEPSCs were averaged as baseline during the 2 min before DHPG application and then again during the last 1 min of the application to assess the magnitude of the drug effect. Field recording pipettes containing ACSF solution were placed in CA3 stratum pyramidale, and experiments were done at 32–35°C with an ACSF perfusion rate of ~5 ml/min. Data were collected with Axopatch 200B or Axopatch 1C amplifiers (Molecular Devices), filtered at 2 kHz, and digitized at 5 kHz with Digidata 1440 or Digidata 1200 (Molecular Devices) and Clampex 9 or 10 software (Molecular Devices).

Chemicals. The membrane-permeable Tat-fused peptides (cf. Mao et al., 2005; Ronesi et al., 2012) mGluR5CT (YGRKKRRQRRR-ALTPPSPFR) and mGluR5MU (YGRKKRRQRRR-ALTPLSPRR) were synthesized at the University of Texas Southwestern Protein Chemistry Technology Center. Peptides were dissolved in water at 5 mM, aliquoted, stored at −20°C, and used at 5 μM. Except for SR141716A [*N*-(Piperidin-1-yl)-5-(4-chlorophenyl)-1-(2,4-dichlorophenyl)-4-methyl-1*H*-pyrazole-3-carboxamide hydrochloride], all drugs were made up as 1000× stocks in distilled water, aliquoted, and frozen at −20°C. SR141716A was made up in DMSO (DMSO bath concentration was 0.02%). Once thawed, aliquots were either used or discarded after 2 months. (*S*)-3,5-DHPG, SR141716A, MPEP, and LY367385 [(*S*)-(+)-α-amino-4-carboxy-2-methylbenzeneacetic acid] were obtained from Tocris Bioscience. NBQX and D-AP-5 were from Ascent Scientific. All other drugs were from Sigma-Aldrich.

Data analysis. χ^2 tests were used to compare proportions. Statistical tests among groups were done with two-way ANOVA. The significance level for all tests was $^*p < 0.05$. Box-and-whisker plots are shown for display purposes. Cumulative distributions were compared with the Kolmogorov–Smirnov (K–S) test (http://www.physics.csbsju.edu/stats/KS-test.n.plot_form.html).

Results

mGluR activation induces synchronized burst discharges more readily in *Fmr1*$^{-/y}$ mice than in WT mice

Bath application of the group I mGluR agonist DHPG (5 μM) to a hippocampal slice from a WT mouse first induced single-unit firing in stratum pyramidale of the CA3 area. In 6 of 21 slices, short synchronized burst discharges (mean ± SEM duration, 153 ± 13 ms; $n = 60$ discharges from 6 slices) began after ~10 min and then occurred regularly with interburst intervals of 2–53 s (Fig. 1*A*). In contrast, in 11 of 12 slices from *Fmr1*$^{-/y}$ mice, 5 μM DHPG induced burst discharges with similar durations (150 ± 11 ms) but shorter interburst intervals than in WT slices ($p < 0.01$, K–S test; $n = 110$ discharges from 11 slices; Fig. 1*B*, *D*, gray line). The difference in probability of burst firing was significant ($p < 0.01$, χ^2 test; Fig. 1*E*). *Fmr1*$^{-/y}$ slices treated with 5 μM DHPG plus the mGluR antagonists LY367385 (10 μM) and MPEP (10 μM) failed to develop bursting, confirming that the bursts result from mGluR activation ($n = 4$). In the 13 of 15 WT slices not showing DHPG-induced bursts within 20 min, subsequent bath application of PTX (100 μM) induced burst firing within 3 min (Fig. 1*A*); the interburst intervals were shorter than in the DHPG-treated slices from *Fmr1*$^{-/y}$ mice ($p < 0.001$, K–S test; $n = 130$ discharges; Fig. 1*D*, thick dashed line). Hence, essentially all WT slices could generate synchronized bursts but were less sensitive to DHPG than *Fmr1*$^{-/y}$ slices.

WT slices with disrupted Homer protein interactions have enhanced burst firing susceptibility

Homer scaffold disruption in WT slices mimics some phenotypes, such as prolonged neocortical up states, of *Fmr1*$^{-/y}$ slices (Ronesi et al., 2012). To determine whether Homer binding disruption mimicked the mGluR hyperexcitability phenotype of *Fmr1*$^{-/y}$, we incubated WT slices with a cell-permeable, Tat-fused peptide having the PPXXF motif of the mGluR5 C-terminal tail (CT peptide) that binds the EVH1 domain of Homer (see Materials and Methods). Control slices received a Tat-fused peptide having a mutated Homer binding motif, the MU peptide, that does not interfere with Homer scaffolds. To confirm that the CT peptide reduced mGluR5–Homer coupling, we used coimmunoprecipitation of mGluR5 and Homer and found (cf. Ronesi et al., 2012) that the CT peptide reduced the coupling to 39 ± 8% of control levels ($n = 3$ animals; $p = 0.005$), whereas the MU peptide was inactive ($n = 3$ animals; $p = 0.55$; data not shown).

In MU peptide-treated slices, short bursts were elicited by DHPG in only 2 of 10 WT slices, similar to untreated WT slices ($p = 0.94$, χ^2 test). However, after CT peptide incubation, 9 of 13 WT slices showed burst discharges ($p < 0.05$, χ^2 test; Fig. 1*C*,*E*), a probability indistinguishable from that of *Fmr1*$^{-/y}$ slices ($p = 0.37$, χ^2 test). In the responsive CT-treated WT slices, synchronized bursts ($n = 90$) had shorter interburst intervals than in the responsive MU-treated slices ($n = 20$; $p < 0.01$, K–S test; Fig. 1*D*, dotted line). Evidently, disruption of Homer scaffold enhances overall excitability.

Homer disruption alters eCB_{mGluR} at hippocampal excitatory and inhibitory synapses

Fmr1$^{-/y}$ slices have increased eCB_{mGluR} activity at inhibitory synapses (Zhang and Alger, 2010). The elevated sensitivity to DHPG-induced burst firing in CT-treated slices, which mimics *Fmr1*$^{-/y}$ hypersensitivity, suggests that Homer disruption might also increase eCB_{mGluR} at inhibitory synapses.

To test this hypothesis, we measured eCB_{mGluR} first in rat hippocampal slices (Fig. 2*A*). At CA1 inhibitory synapses, 2, 5, 10, and 20 μM DHPG, applied for 3–4 min, reversibly reduced eIPSCs by 13 ± 4, 22 ± 3, 47 ± 5, and 63 ± 6%, respectively ($n = 5$ for each concentration). CT peptide treatment significantly enhanced the DHPG effects at 2, 5, and 10 μM (Fig. 2*B*), with the eIPSCs being inhibited by 27 ± 3, 54 ± 4, and 65 ± 5%, respectively ($n > 8$; $p < 0.001$, two-way ANOVA). At 20 μM, DHPG reduced eIPSCs by 72 ± 6% ($n = 7$), similar to control, indicating a ceiling effect. Such short-term mGluR activation avoids LTD induction (cf. Heifets and Castillo, 2009). The MU peptide did not affect eCB_{mGluR} (11 ± 3, 24 ± 4, 52 ± 4, and 59 ± 4% for 2, 5, 10, and 20 μM DHPG, respectively; $n > 6$; $p = 0.75$, two-way ANOVA). Finally, the CB_1R antagonist SR141716A, at 5 μM (slices pretreated for >2 h), abolished the effects of DHPG in CT peptide-treated slices ($n = 4$).

We also tested the effects of Homer disruption on Ca^{2+}-induced eCB mobilization by measuring depolarization-induced suppression of inhibition (DSI) in pyramidal neurons. Depolarization steps from −70 to 0 mV lasting 0.5, 1, or 2 s reduced eIPSC amplitudes to the same extent in rat slices treated with either CT or MU peptides (by 33 ± 4, 43 ± 5, and 55 ± 5% for CT and 31 ± 4, 43 ± 3, and 49 ± 5% for MU, respectively; $n > 9$ for CT and $n > 7$ for MU; $p = 0.16$). Although DSI is an eCB- and CB_1R-dependent process, it is produced solely by a rise in $[Ca^{2+}]_i$ and uses biochemical pathways distinct from those of eCB_{mGluR} (Kano et al., 2009). The negative results on DSI demonstrate that the CT peptide does not affect CB_1R function, eCB release from pyramidal cells, or the coupling between the rise in postsynaptic $[Ca^{2+}]_i$ and eCB mobilization. Importantly, DSI is also unaffected in *Fmr1*$^{-/y}$ CA1 (Zhang and Alger, 2010).

Compared with its effects on eIPSCs, DHPG had relatively weak effects on eEPSCs, and only at doses ≥20 μM did it significantly inhibit eEPSCs, decreasing them by 23 ± 6 and 39 ± 3% at 20 and 50 μM, respectively (Figs. 2*E*,*F*). Nevertheless, in CT-treated slices, the DHPG-induced inhibition of eEPSCs was significantly reduced (to 7 ± 2 and 14 ± 4% at 20 and 50 μM, respectively; $n = 4$; $p < 0.001$, two-way ANOVA). Thus, Homer disruption has two diametrically opposed effects: it enhances eCB_{mGluR} at inhibitory synapses but decreases eCB_{mGluR} at excitatory synapses. Although both effects would normally shift the excitation/inhibition balance toward excitation, because 5 μM DHPG did not significantly affect the amplitudes of eEPSCs in either condition (Fig. 2*F*), the shift of the excitation/inhibition balance caused by the peptide at this low concentration of DHPG is attributable to its effects on inhibitory synapses.

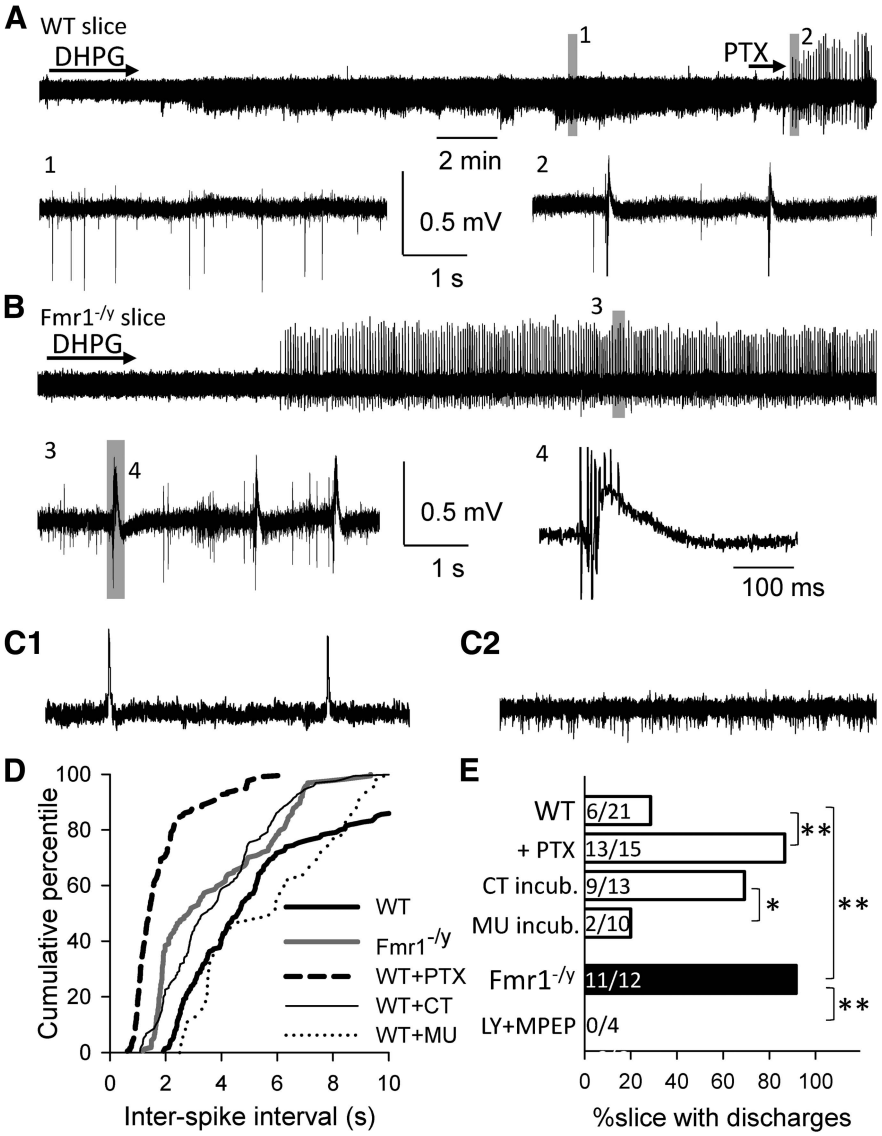

Figure 1. A low concentration of DHPG induces epileptic burst discharges in the CA3 region of hippocampal slices from *Fmr1*$^{-/y}$ mice. ***A***, Field recording in CA3 stratum pyramidale of a WT mouse hippocampal slice after addition of 5 μM DHPG in the perfusate. Generally, DHPG induced strong single-unit discharges, but not synchronized activity, until 100 μM PTX was added. ***B***, In most slices from *Fmr1*$^{-/y}$ mice, 5 μM DHPG induced synchronized activity within 20 min. ***C***, CA3 field recordings after DHPG application for 15 min in WT slices preincubated with Homer scaffold disrupting CT peptide (***C1***) and control MU peptide (***C2***). ***D***, Interspike intervals of the synchronized discharges in slices under different conditions. ***E***, Probability of synchronized discharge induction by DHPG under various conditions. LY, LY367385. *$p < 0.05$, **$p < 0.01$.

Disruption of Homer scaffold fails to enhance eCB signal in *Fmr1*$^{-/y}$ slices

In *Fmr1*$^{-/y}$ mice, the coupling between mGluR5 and structural Homer proteins is decreased (Ronesi and Huber, 2008) and therefore the CT peptide does not increase the severity of the Homer scaffold-dependent *Fmr1*$^{-/y}$ phenotype (Ronesi et al., 2012). If there is a link between Homer proteins and *Fmr1* dele-

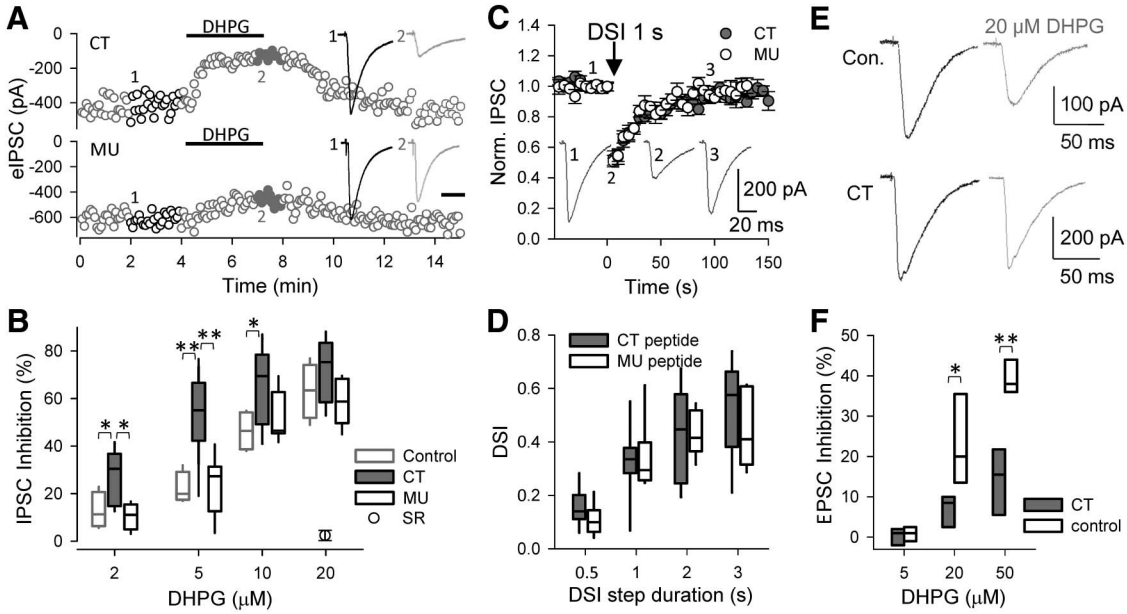

Figure 2. CT peptide enhances DHPG-induced eCB inhibition of eIPSCs. ***A***, Responses of eIPSCs to 5 μM DHPG (3 min application) in rat slices treated with CT (top) or MU (bottom) peptides. ***B***, Pooled data of DHPG-induced inhibition of IPSCs. Note that the CB_1R antagonist SR141716A (5 μM; SR) completely blocked the DHPG-induced inhibition (circle). ***C***, Suppression of eIPSCs in response to 1 s depolarization of postsynaptic pyramidal neurons to 0 mV (DSI) in peptide-treated rat slices. ***D***, Pooled DSI data in response to a range of depolarization durations. ***E***, Responses of eEPSCs to 20 μM DHPG in rat slices. ***F***, Pooled data of DHPG-induced inhibition of eEPSCs. Note that neither 5 μM DHPG nor the CT peptide had significant effect on eEPSCs, whereas CT treatment suppressed the eEPSC inhibition produced by higher DHPG concentrations. $*p < 0.05$, $**p < 0.01$.

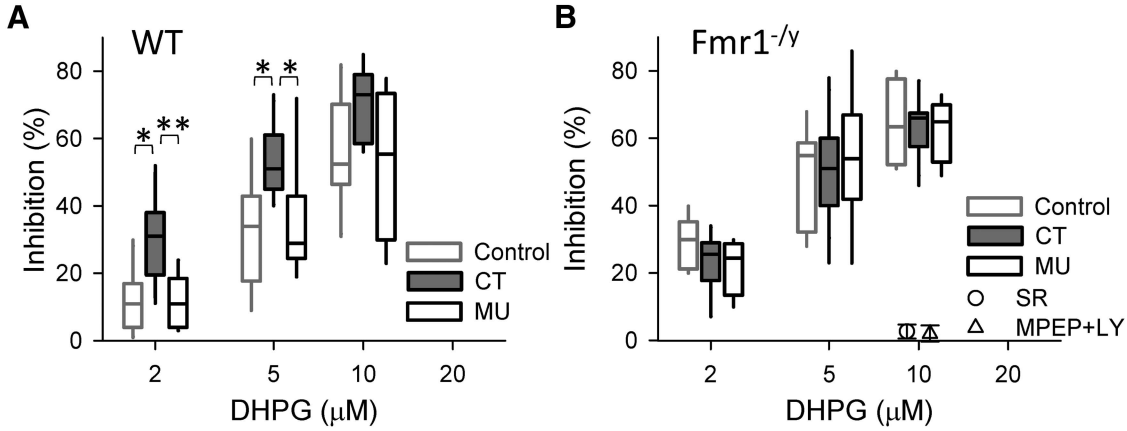

Figure 3. CT peptide enhances DHPG-induced eCB inhibition of eIPSCs in slices from WT mice (***A***) but not *Fmr1*$^{-/y}$ mice (***B***). Note that 5 μM DHPG-induced inhibition of IPSCs was fully blocked by the CB_1R antagonist SR141716A (5 μM; circle) or the group I mGluR antagonists MPEP (10 μM) and LY367385 (10 μM; triangle). $*p < 0.05$, $**p < 0.01$.

tion related to eCB mobilization, the effects of the CT peptide on eCB_{mGluR} should be occluded in *Fmr1*$^{-/y}$ tissue.

To test this prediction, we first replicated the enhancing effect of the CT peptide on eCB_{mGluR} in WT mouse slices. DHPG at 2, 5, and 10 μM reduced eIPSCs by11 ± 3, 33 ± 5, and 56 ± 5%, respectively ($n > 7$; Fig. 3*A*) in the control slices. In contrast, in the presence of the CT peptide, DHPG reduced the eIPSCs by 30 ± 3, 52 ± 3, and 70 ± 5%, respectively, i.e., a highly significant enhancement of inhibition ($n > 8$; $p < 0.001$, two-way ANOVA), whereas the MU peptide had no effect on DHPG-induced inhibition (12 ± 3, 35 ± 6, and 53 ± 2%, respectively; $n > 6$; $p = 0.57$, two-way ANOVA). In slices from *Fmr1*$^{-/y}$ mice, DHPG at 2, 5, and 10 μM reduced eIPSCs by 23 ± 3, 50 ± 4, and 63 ± 3%, respectively, which was significantly more than in WT slices ($n > 9$; $p < 0.001$, two-way ANOVA) but not different from the inhibition in CT peptide-treated WT slices ($p = 0.42$, two-way ANOVA; Fig. 3*A*).

Most importantly, incubation of *Fmr1*$^{-/y}$ slices with either the CT or MU peptides did not change the DHPG-induced reduction of eIPSCs (22 ± 3, 53 ± 8, and 62 ± 4% for CT and 29 ± 3, 49 ± 5, and 65 ± 7% for MU, respectively; $n > 7$; $p > 0.05$, two-way ANOVA). Finally, either 5 μM SR141716A or a combination of 10 μM MPEP and 10 μM LY367385 abolished the effects of 10 μM DHPG in CT peptide-treated *Fmr1*$^{-/y}$ slices ($n = 3$), confirming that DHPG reduced the eIPSCs via eCB_{mGluR}.

CB_1R antagonism suppresses DHPG-induced burst firing

We hypothesized that the heightened epileptiform burst susceptibility of *Fmr1*$^{-/y}$ slices is attributable to eCB_{mGluR}-induced excitatory/inhibitory imbalance, which predicts that CB_1R blockade would reverse the imbalance and prevent burst firing. To test this prediction, we incubated *Fmr1*$^{-/y}$ slices with 5 μM SR141716A to block CB_1Rs before applying 5 μM DHPG. No field potential bursts were observed in 12 of 13 SR141716A-

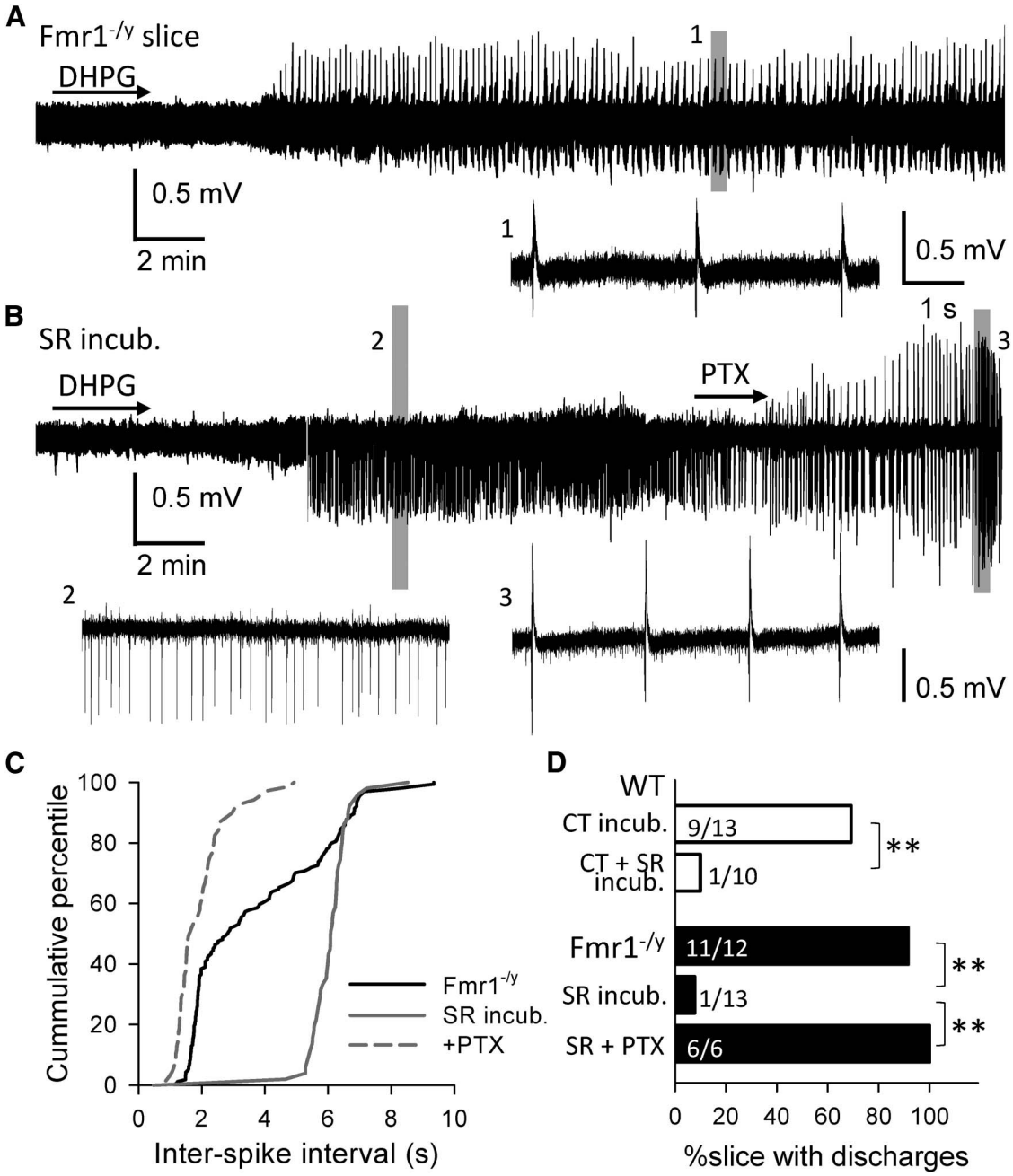

Figure 4. Low concentration of DHPG induces population burst firing in *Fmr1*$^{-/y}$ slices that depends on eCBs. ***A***, Field recording of activity induced by 5 μM DHPG in CA3 stratum pyramidale of an *Fmr1*$^{-/y}$ mouse hippocampal slice. ***B***, Responses of an *Fmr1*$^{-/y}$ slice preincubated with the CB_1R antagonist SR141716A to DHPG and PTX. Note the DHPG-induced strong single-unit discharges, but absence of burst firing, before PTX application. ***C***, Interspike intervals of the burst discharges in slices. ***D***, Probability of DHPG-induced burst discharges in slices under different conditions. Blockade of CB_1Rs greatly suppressed the epileptic activity in both *Fmr1*$^{-/y}$ and CT-treated WT slices. SR, SR141716A. *$p < 0.05$, **$p < 0.01$.

treated slices within 20 min after DHPG application, although asynchronous single-unit spike firing was greatly enhanced (Fig. 4*B*). In the slice in which bursting occurred, the interburst intervals were much longer than normal ($n = 20$ discharges; $p < 0.01$, K–S test; Fig. 4*C*). Restoring the excitatory/inhibitory imbalance by blocking all inhibitory synaptic transmission with 100 μM PTX reinstated the epileptic activity in all six of the nonresponsive slices tested ($p < 0.001$, χ^2 test; Figs. 4*B*,*D*). In CT-treated WT slices, SR141716A incubation also greatly suppressed the epileptogenesis ($p < 0.001$, χ^2 test; Fig. 4*D*): DHPG-induced synchronized bursts in only 1 of 10 slices, and the interburst intervals were longer than normal ($n = 20$ discharges; $p < 0.01$, K–S test).

Discussion

We report novel findings on excitability control in the FXS mouse model. (1) Disruption of Homer scaffolds increased group I mGluR-stimulated epileptiform discharges (Chuang et al., 2005) whether the disruption was caused by the deletion of *Fmr1* or a membrane-permeable CT peptide. (2) Antagonism of CB_1R activity prevented development of hyperexcitability in both models, implying that the eCB system was affected by disruption of mGluR–Homer interactions. (3) The CT peptide enhanced eCB_{mGluR} at inhibitory synapses but decreased it at excitatory synapses, exactly replicating observations in the *Fmr1*$^{-/y}$ mouse,

in which eCB_{mGluR} is increased at inhibitory (Maccarrone et al., 2010; Zhang and Alger, 2010) and decreased at excitatory (Jung et al., 2012) synapses.

The alterations of eCB_{mGluR} in *Fmr1*$^{-/y}$ are probably related to changes in Homer binding, because Homer 1a overexpression also decreases eCB_{mGluR} at excitatory synapses in cell cultures (Roloff et al., 2010). The molecular organization of the eCB_{mGluR} system is well understood at excitatory synapses (Lafourcade et al., 2007; Katona and Freund, 2008). There, the decrease in eCB_{mGluR} in *Fmr1*$^{-/y}$ is attributed to translocation of Diacylglycerol lipase-alpha (DGLα) to spine necks from its usual position near perisynaptic mGluRs in the spine head (Jung et al., 2012). Homers are required to localize DGLα near the plasma membrane (Jung et al., 2007) and facilitate detection of eCB_{mGluR} signaling in expression systems (Won et al., 2009). It is likely that disrupted Homer binding accounts for the abnormal positioning of DGLα in *Fmr1*$^{-/y}$ (Jung et al., 2012), although this has not been tested. Importantly, no alteration in DGLα localization was observed at inhibitory synapses (Jung et al., 2012). Indeed, the molecular complex that generates eCBs at perisomatic inhibitory synapses is not known. Finding that eCB_{mGluR} is increased at perisomatic inhibitory synapses by the CT peptide and in *Fmr1*$^{-/y}$ tissue (Maccarrone et al., 2010; Zhang and Alger, 2010) suggests that the intact Homer scaffold ordinarily opposes full eCB_{mGluR} expression at these synapses (Fig. 2*B*).

The densities of both mGluR5 and DGLα are much lower in pyramidal cell somata than dendrites (Katona et al., 2006; Yoshida et al., 2006; Kano et al., 2009). These observations, together with the absence of somatic glutamatergic terminals, suggest that 2-arachidonoylglycerol (2-AG) from dendritic regions could diffuse back and affect perisomatic inhibitory terminals. In this case, disruption of Homer scaffolds would change the localization of mGluR5 and/or DGLα in spines or dendrites to favor 2-AG diffusion toward somata. However, the presence of active uptake and degradation systems (Kano et al., 2009), together with evidence that dendritically produced 2-AG cannot diffuse more than ~10 μm (Chevaleyre and Castillo, 2004), argues that dendritic 2-AG spillover cannot reach perisomatic synapses. Alternatively, despite their low densities, mGluR5 and DGLα in somata may mobilize sufficient 2-AG locally via glutamate spillover from dendrites or astrocytes in stratum pyramidale. The higher concentrations of CB_1Rs on somatic terminals makes them much more sensitive to eCBs than dendritic terminals (Kano et al., 2009). Bath application of group I mGluR agonists or inhibition of glutamate uptake enhances DSI (Morishita and Alger, 1999), mediated by the somatic eCB_{mGluR} system.

The enhancing effect of Homer disruption at inhibitory synapses could reflect a different basal arrangement of Homer–mGluR5 coupling on somata. For example, Homer disruption could release mGluR5 from binding to other proteins, increasing its availability to stimulate 2-AG synthesis. Interestingly, activation of DGLα is independent of Homer binding; DGLα generates 2-AG equally well when Homer binding is prevented (Jung et al., 2007). Fully understanding the Homer modulation of eCB_{mGluR} at perisomatic inhibitory synapses will require elucidating the molecular organization of the eCB_{mGluR} system.

Other Homer binding partners, including DGLα, have the same proline-rich binding motif (PPXXF) found in mGluR5 (Jung et al., 2007). The CT peptide could disrupt coupling of Homer to these partners as well. Homer proteins act collectively as a molecular switch that reprioritizes mGluR signaling, with some mGluR-mediated processes being inhibited and some facilitated by Homers (Kammermeier, 2008; Won et al., 2009). The CT peptide does not reduce Homer or mGluR levels, membrane localization, activation of phospholipase C, elevation of intracellular Ca^{2+} (Mao et al., 2005), or basal synaptic transmission (Ronesi and Huber, 2008; Ronesi et al., 2012), and we show that the CT peptide also does not affect DSI, i.e., that it has no effect on $GABA_A$ receptors, Ca^{2+} influx, eCB release, or binding to CB_1Rs. CT peptide-mediated Homer scaffold disruption mimics some phenotypical features of *Fmr1*$^{-/y}$ in WT neocortical slices (Ronesi et al., 2012), and CT has little effect in *Fmr1*$^{-/y}$ neocortex, as expected if Homer-dependent interactions are already compromised. Thus, it is reasonable to attribute CT peptide effects to disruption of Homer scaffolds. In the hippocampus, depolarization-induced suppression of excitation (DSE) is markedly weaker than DSI and difficult to measure (Wagner and Alger, 1996; Ohno-Shosaku et al., 2002). The biochemical mechanisms of DSE and DSI appear to be identical (Hashimotodani et al., 2005; Tanimura et al., 2010); hence, it is likely that DSE is unchanged by Homer modulation, although this should be tested in tissue with robust DSE (e.g., cerebellum; Kreitzer and Regehr, 2001).

The ability of DHPG to induce eCB LTD is very sensitive to experimental details, especially concentration and duration of DHPG application. Generally, high concentrations and long durations are needed for eCB LTD at CA1 excitatory synapses (Xu et al., 2010; Péterfi et al., 2012). However, others (Rouach and Nicoll, 2003; Nosyreva and Huber, 2005) failed to observe an eCB_{mGluR}-dependent component of LTD under conditions like ours, suggesting that technical details may account for variability in observing eCB LTD. At CA1 perisomatic inhibitory synapses, we showed (Zhang and Alger, 2010) that normally 5 μM DHPG produces reversible IPSC suppression, whereas 50 μM is required for eCB LTD, but that in the *Fmr1*$^{-/y}$ mouse, 5 μM DHPG does induce LTD. Here, we applied DHPG for only 3–4 min to eIPSCs and 5 min to eEPSCs to avoid inducing LTD so that we could efficiently assess the inhibition caused by different concentrations of DHPG. eCB LTD remains to be studied.

Seizure susceptibility is increased in *Fmr1*$^{-/y}$ mice and FXS patients (Musumeci et al., 1999). We investigated the brief epileptiform burst potentials elicited with low DHPG concentrations. These brief bursts resemble the short bursts emerging immediately after mGluR activation by high concentrations of DHPG or $GABA_A$ receptor blockade (Chuang et al., 2005). We did not observe the prolonged epileptiform bursts, even 1 h after DHPG application, probably because we used low DHPG concentrations, a lower experimental temperature, and a submersion-type chamber (rather than an interface-type chamber; cf. Chuang et al., 2005). It will be important to examine CB_1R sensitivity of the prolonged mGluR-induced discharges produced by high DHPG concentrations in *Fmr1*$^{-/y}$ (Chuang et al., 2005).

Broadly speaking, seizures arise from an imbalance of excitation and inhibition toward excitation, and the underlying mechanisms may include alterations in the strength of excitatory and/or inhibitory synapses, neuronal network oscillations, and rewiring of neuronal circuits. Although CB_1Rs exist on both excitatory and inhibitory synaptic terminals, their density in the hippocampus is much higher at inhibitory terminals (Katona and Freund, 2008; Kano et al., 2009). Hence, widespread action of eCBs may suppress inhibition more than excitation and thereby promote hyperexcitability. This may be particularly important when eCB mobilization occurs, such as with group I mGluR activation. Hippocampal pyramidal cells densely express group I

mGluRs, and, in response to DHPG application, these neurons fire action potentials (Fig. 1*A*). Meanwhile, as we have shown, DHPG at a low concentration suppresses perisomatic inhibitory transmission but has no effect on excitatory synapses (Fig. 2). This will push the neuronal circuit toward its limit in maintaining normal excitability. Any additional shift toward excitation, such as additional eCB mobilization by higher DHPG, Homer disruption (Fig. 1), or Fmr1 malfunction (Fig. 1; Ronesi et al., 2012), will greatly increase the chance of epileptogenesis. Importantly, a similar increase in eCB signaling at GABAergic synapses has been reported in a febrile seizure model (Chen et al., 2007), and blockade of CB_1Rs reduced epileptiform activity there. However, these results differ from those obtained with the kainic acid model in which eCB actions on hippocampal glutamatergic nerve terminals are the most important for neuroprotection (Monory et al, 2006). The difference may be explained by the fact that kainic acid inhibits GABA release (Fisher and Alger, 1984; Carta et al. 2014) including GABA release from CB1R+ interneurons (Lourenco et al., 2010). Kainic acid suppression of this inhibition will contribute to epileptogenic activity, and by depressing release from CB1R+ interneurons, also occlude the influence of eCBs on inhibition in this seizure model.

Our results suggest that at least the early stages of hyperexcitability associated with excessive eCB actions in FXS could be reversed by CB_1R antagonism rather than by their activation. Indeed, numerous phenotypic features of $Fmr1^{-/y}$ mice, including their elevated audiogenic seizure susceptibility, can be reversed by genetic elimination or pharmacological blockade of CB_1Rs (Busquets-Garcia et al., 2013). We suggest that related therapeutic opportunities in FXS may be associated with the Homer scaffold system.

References

Bear MF, Huber KM, Warren ST (2004) The mGluR theory of fragile X mental retardation. Trends Neurosci 27:370–377. CrossRef Medline

Bianchi R, Chuang SC, Zhao W, Young SR, Wong RK (2009) Cellular plasticity for group I mGluR-mediated epileptogensis. J Neurosci 29:3497–3507. CrossRef Medline

Busquets-Garcia A, Gomis-González M, Guegan T, Agustín-Pavón C, Pastor A, Mato S, Pérez-Samartín A, Matute C, de la Torre R, Dierssen M, Maldonado R, Ozaita A (2013) Targeting the endocannabinoid system in the treatment of fragile X syndrome. Nat Med 19:603–607. CrossRef Medline

Carta M, Fièvre S, Gorlewicz A, Mulle C. (2014) Kainate receptors in the hippocampus. Eur J Neurosci 39:1835–1844. CrossRef Medline

Chen K, Neu A, Howard AL, Földy C, Echegoyen J, Hilgenberg L, Smith M, Mackie K, Soltesz I (2007) Prevention of plasticity of endocannabinoid signaling inhibits persistent limbic hyperexcitability caused by developmental seizures. J Neurosci 27:46–58. CrossRef Medline

Chevaleyre V, Castillo PE (2004) Endocannabinoid-mediated metaplasticity in the hippocampus. Neuron 43:871–881. CrossRef Medline

Chuang SC, Zhao W, Bauchwitz R, Yan Q, Bianchi R, Wong RK (2005) Prolonged epileptiform discharges induced by altered group I metabotropic glutamate receptor-mediated synaptic responses in hippocampal slices of a fragile X mouse model. J Neurosci 25:8048–8055. CrossRef Medline

Darnell JC, Klann E (2013) The translation of translational control by FMRP: therapeutic targets for FXS. Nat Neurosci 16:1530–1536. CrossRef Medline

Dölen G, Osterweil E, Rao BS, Smith GB, Auerbach BD, Chattarji S, Bear MF (2007) Correction of fragile X syndrome in mice. Neuron 56:955–962. CrossRef Medline

Fisher RS, Alger BE (1984) Electrophysiological mechanisms of kainic acid-induced epileptiform activity in the rat hippocampal slice. J Neurosci 4:1312–1323. Medline

Freund TF, Katona I (2007) Perisomatic inhibition. Neuron 56:33–42. CrossRef Medline

Giuffrida R, Musumeci S, D'Antoni S, Bonaccorso CM, Giuffrida-Stella AM, Oostra BA, Catania MV (2005) A reduced number of metabotropic glutamate subtype 5 receptors are associated with constitutive homer proteins in a mouse model of fragile X syndrome. J Neurosci 25:8908–8916. CrossRef Medline

Hashimotodani Y, Ohno-Shosaku T, Tsubokawa H, Ogata H, Emoto K, Maejima T, Araishi K, Shin HS, Kano M (2005) Phospholipase Cbeta serves as a coincidence detector through its Ca2+ dependency for triggering retrograde endocannabinoid signal. Neuron 45:257–268. CrossRef Medline

Heifets BD, Castillo PE (2009) Endocannabinoid signaling and long-term synaptic plasticity. Annu Rev Physiol 71:283–306. CrossRef Medline

Jung KM, Astarita G, Zhu C, Wallace M, Mackie K, Piomelli D (2007) A key role for diacylglycerol lipase-alpha in metabotropic glutamate receptor-dependent endocannabinoid mobilization. Mol Pharmacol 72:612–621. CrossRef Medline

Jung KM, Sepers M, Henstridge CM, Lassalle O, Neuhofer D, Martin H, Ginger M, Frick A, DiPatrizio NV, Mackie K, Katona I, Piomelli D, Manzoni OJ (2012) Uncoupling of the endocannabinoid signalling complex in a mouse model of fragile X syndrome. Nat Commun 3:1080. CrossRef Medline

Kammermeier PJ (2008) Endogenous homer proteins regulate metabotropic glutamate receptor signaling in neurons. J Neurosci 28:8560–8567. CrossRef Medline

Kano M, Ohno-Shosaku T, Hashimotodani Y, Uchigashima M, Watanabe M (2009) Endocannabinoid-mediated control of synaptic transmission. Physiol Rev 89:309–380. CrossRef Medline

Katona I, Freund TF (2008) Endocannabinoid signaling as a synaptic circuit breaker in neurological disease. Nat Med 14:923–930. CrossRef Medline

Katona I, Urbán GM, Wallace M, Ledent C, Jung KM, Piomelli D, Mackie K, Freund TF (2006) Molecular composition of the endocannabinoid system at glutamatergic synapses. J Neurosci 26:5628–5637. CrossRef Medline

Klugmann M, Szumlinski KK (2008) Targeting Homer genes using adeno-associated viral vector: lessons learned from behavioural and neurochemical studies. Behav Pharmacol 19:485–500. CrossRef Medline

Kreitzer AC, Regehr WG (2001) Retrograde inhibition of presynaptic calcium influx by endogenous cannabinoids at excitatory synapses onto Purkinje cells. Neuron 29:717–727. CrossRef Medline

Lafourcade M, Elezgarai I, Mato S, Bakiri Y, Grandes P, Manzoni OJ (2007) Molecular components and functions of the endocannabinoid system in mouse prefrontal cortex. PLoS One 2:e709. Medline

Lenz RA, Wagner JJ, Alger BE. (1998) N- and L-type calcium channel involvement in depolarization-induced suppression of inhibition in rat hippocampal CA1 cells. J Physiol 512:61–73. CrossRef Medline

Lourenço J, Cannich A, Carta M, Coussen F, Mulle C, Marsicano G. (2010) Synaptic activation of kainate receptors gates presynaptic CB(1) signaling at GABAergic synapses. Nat Neurosci 13:197–204. CrossRef Medline

Maccarrone M, Rossi S, Bari M, De Chiara V, Rapino C, Musella A, Bernardi G, Bagni C, Centonze D (2010) Abnormal mGlu 5 receptor/endocannabinoid coupling in mice lacking FMRP and BC1 RNA. Neuropsychopharmacol 35:1500–1509. CrossRef Medline

Mao L, Yang L, Tang Q, Samdani S, Zhang G, Wang JQ (2005) The scaffold protein Homer1b/c links metabotropic glutamate receptor 5 to extracellular signal-regulated protein kinase cascades in neurons. J Neurosci 25:2741–2752. CrossRef Medline

Monory K, Massa F, Egertová M, Eder M, Blaudzun H, Westenbroek R, Kelsch W, Jacob W, Marsch R, Ekker M, Long J, Rubenstein JL, Goebbels S, Nave KA, During M, Klugmann M, Wölfel B, Dodt HU, Zieglgänsberger W, Wotjak CT, et al. (2006) The endocannabinoid system controls key epileptogenic circuits in the hippocampus. Neuron 51:455–466. CrossRef Medline

Morishita W, Alger BE (1999) Evidence for endogenous excitatory amino acids as mediators in DSI of GABA(A)ergic transmission in hippocampal CA1. J Neurophysiol 82:2556–2564. Medline

Morishita W, Kirov SA, Alger BE (1998) Evidence for metabotropic glutamate receptor activation in the induction of depolarization-induced suppression of inhibition in hippocampal CA1. J Neurosci 18:4870–4882. Medline

Musumeci SA, Hagerman RJ, Ferri R, Bosco P, Dalla Bernardina B, Tassinari CA, De Sarro GB, Elia M (1999) Epilepsy and EEG findings in males with fragile X syndrome. Epilepsia 40:1092–1099. CrossRef Medline

Nosyreva ED, Huber KM (2005) Developmental switch in synaptic mecha-

nisms of hippocampal metabotropic glutamate receptor-dependent long-term depression. J Neurosci 25:2992–3001. CrossRef Medline

Ohno-Shosaku T, Tsubokawa H, Mizushima I, Yoneda N, Zimmer A, Kano M (2002) Presynaptic cannabinoid sensitivity is a major determinant of depolarization-induced retrograde suppression at hippocampal synapses. J Neurosci 22:3864–3872. Medline

Olmos-Serrano JL, Paluszkiewicz SM, Martin BS, Kaufmann WE, Corbin JG, Huntsman MM (2010) Defective GABAergic neurotransmission and pharmacological rescue of neuronal hyperexcitability in the amygdala in a mouse model of fragile X syndrome. J Neurosci 30:9929–9938. CrossRef Medline

Osterweil EK, Chuang SC, Chubykin AA, Sidorov M, Bianchi R, Wong RK, Bear MF (2013) Lovastatin corrects excess protein synthesis and prevents epileptogenesis in a mouse model offragile X syndrome. Neuron 77:243–250. CrossRef Medline

Paluszkiewicz SM, Martin BS, Huntsman MM (2011) Fragile X syndrome: the GABAergic system and circuit dysfunction. Dev Neurosci 33:349–364. CrossRef Medline

Péterfi Z, Urbán GM, Papp OI, Németh B, Monyer H, Szabó G, Erdélyi F, Mackie K, Freund TF, Hájos N, Katona I (2012) Endocannabinoid-mediated long-term depression of afferent excitatory synapses in hippocampal pyramidal cells and GABAergic interneurons. J Neurosci 32: 14448–14463. CrossRef Medline

Roloff AM, Anderson GR, Martemyanov KA, Thayer SA (2010) Homer 1a gates the induction mechanism for endocannabinoid-mediated synaptic plasticity. J Neurosci 30:3072–3081. CrossRef Medline

Ronesi JA, Huber KM (2008) Homer interactions are necessary for metabotropic glutamate receptor-induced long-term depression and translational activation. J Neurosci 28:543–547. CrossRef Medline

Ronesi JA, Collins KA, Hays SA, Tsai NP, Guo W, Birnbaum SG, Hu JH, Worley PF, Gibson JR, Huber KM (2012) Disrupted Homer scaffolds mediate abnormal mGluR5 function in a mouse model of fragile X syndrome. Nat Neurosci 15:431–440, S1. CrossRef Medline

Rouach N, Nicoll RA (2003) Endocannabinoids contribute to short-term but not long-term mGluR-induced depression in the hippocampus. Eur J Neurosci 18:1017–1020. CrossRef Medline

Tanimura A, Yamazaki M, Hashimotodani Y, Uchigashima M, Kawata S, Abe M, Kita Y, Hashimoto K, Shimizu T, Watanabe M, Sakimura K, Kano M (2010) The endocannabinoid 2-arachidonoylglycerol produced by diacylglycerol lipase alpha mediates retrograde suppression of synaptic transmission. Neuron 65:320–327. CrossRef Medline

Varma N, Carlson GC, Ledent C, Alger BE (2001) Metabotropic glutamate receptors drive the endocannabinoid system in hippocampus. J Neurosci 21:RC188(1–5). Medline

Wagner JJ, Alger BE (1996) Increased neuronal excitability during depolarization-induced suppression of inhibition in rat hippocampus. J Physiol 495:107–112. CrossRef Medline

Wilson RI, Kunos G, Nicoll RA (2001) Presynaptic specificity of endocannabinoid signaling in the hippocampus. Neuron 31:453–62. CrossRef

Won YJ, Puhl HL 3rd, Ikeda SR (2009) Molecular reconstruction of mGluR5a-mediated endocannabinoid signaling cascade in single rat sympathetic neurons. J Neurosci 29:13603–13612. CrossRef Medline

Xu JY, Chen R, Zhang J, Chen C (2010) Endocannabinoids differentially modulate synaptic plasticity in rat hippocampal CA1 pyramidal neurons. PLoS One 5:e10306. CrossRef Medline

Yoshida T, Fukaya M, Uchigashima M, Miura E, Kamiya H, Kano M, Watanabe M (2006) Localization of diacylglycerol lipase-α around postsynaptic spine suggests close proximity between production site of an endocannabinoid, 2-arachidonoyl-glycerol, and presynaptic cannabinoid CB1 receptor. J Neurosci 26:4740–4751. CrossRef Medline

Zhang L, Alger BE (2010) Enhanced endocannabinoid signaling elevates neuronal excitability in fragile X syndrome. J Neurosci 30:5724–5729. CrossRef Medline

Zhao W, Chuang SC, Bianchi R, Wong RK (2011) Dual regulation of fragile X mental retardation protein by group I metabotropic glutamate receptors controls translation-dependent epileptogenesis in the hippocampus. J Neurosci 31:725–734. CrossRef Medline